Multi-temporal Optimal Power Flow for Assessing the Renewable Generation Hosting Capacity of an Active Distribution System

Etta Grover-Silva, Robin Girard, Georges Kariniotakis

Multi-temporal Optimal Power Flow for Assessing the Renewable Generation Hosting Capacity of an Active Distribution System

Etta Grover-Silva*, Robin Girard*, George Kariniotakis*, *SMIEEE*
*MINES ParisTech, PSL - Research University, PERSEE - Center for Processes, Renewable Energies and Energy Systems
06904 Sophia Antipolis, France
Email: etta.grover-silva@mines-paristech.fr

***Abstract*—The detailed modeling of distribution grids is expected to be critical to understand the current functionality limits and necessary retrofits to satisfy integration of massive amounts of distributed generation, energy storage devices and the electric consumption demand of the future. Due to the highly dimensional non-convex characteristics of the power flow equations, convex relaxations have been used to ensure an efficient calculation time. However, these relaxations have been proven to be inexact during periods of high RES injection. In this paper additional linear constraints were introduced in the power flow formulation to guaranty an exact relaxation. This convex relaxation is then applied within a multi-temporal algorithm in order to evaluate the benefits of storage grid integration. The case study of a French medium voltage feeder is studied to evaluate the maximum capacity of the grid to host RES sources and the advantages of storage systems in reducing curtailment of RES.**

I. Introduction

The electric distribution system is critical for energy security and economic stability. With the exploration of new energy production solutions including renewable energy sources (RES) and associated storage devices, the architecture and functionality of the current distribution grid has been a subject of high interest. For example, a renewable energy source could include wind turbines, hydro turbines or photovoltaic panels. The simulation of current functionality limits with new decentralized renewable energy generation can in turn indicate the advantages of the automation and control of components in the distribution grid. This automation and control is typically labeled as an active distribution system. The added control possibilities of an active distribution grid can allow for a high capacity of decentralized generators to be installed without major infrastructure upgrades. The capacity of a grid to integrate decentralized generators without violating operational limits can be called a distribution grid hosting capacity. In order to quantify the hosting capacity of a distribution grid, detailed AC power flow models are necessary. However, for AC power flow algorithms to be useful and applicable, computation time must be optimized.

There exists many different techniques of AC power flow modeling. However, power flow calculations are non-linear, non-convex and highly dimensional, which can be extremely computationally intensive. Existing power flow algorithms include the forward/backward sweep, Newton Raphson method [1], [2], fast-decoupled load-flow method [3], [4], z-bus matrix construction method [5], and loop impedance method [6], [7]. The quantification of the current hosting capacity of the electric grid is evaluated in [8]. As noted within this study, possible strategies to increase this current hosting capacity include curtailment and dynamic line rating. Other strategies well explored in the literature include the use of storage elements [9].

The development of smart grid solutions and grid automation has increased the passive hosting capacity by controlling certain components during critical times. However, management algorithms for optimal control must resolve this highly dimensional non-convex power flow problem. Convex optimum power flow relaxation algorithms have been developed to optimize the controllable components while ensuring algorithmic efficiency as seen in [10], [11]. Heuristic methods have also been explored to solve the non-convex power flow equations as seen in [12]. However, heuristic algorithms often require a larger calculation burden as noted in [13] when compared to convex relaxation algorithms. The family of convex relaxation algorithms that is most commonly used for distribution grids is called a Quadratically Constrained Quadratic Program (QCQP). In multiple studies, the non-convex power flow equations have been cast as a QCQP as shown in [14], [15]. Within the QCQP family, two convex relaxation algorithms exist including the Second-Order Cone Program (SOCP) or the Semi-Definite Program (SDP). An SDP convex relaxation has been proved to be exact under certain conditions by [16]. While an SOCP relaxation has also proved to be exact under certain conditions as stated in [17], [10], [18]. However, these relaxations have been proven to be inexact during periods of high renewable energy production feeding into the grid due to elevated line losses [19]. In order to determine the hosting capacity of a distribution grid, it is critical to have a precise and accurate calculation methodology when RE production is high. An example of this difficulty could be high photovoltaic (PV) production during the summer season. In order to overcome the challenge of inaccurate results at periods of high PV injection, [19] presents an AC optimum power flow algorithm that integrates linear cuts implemented in a iterative fashion to ensure an exact and feasible relaxation of the power flow equations. This single phase AC optimum power flow algorithm minimizes losses in the system, while also minimizing the distance between the curtailed production and the real PV production capacity. This methodology allows for the instantaneous assessment of grid operational limits with a certain PV injection and a certain consumption. However, this algorithm does not allow for the assessment of time dependent components such as storage devices. In contrast to the literature, the consideration of multiple time steps permits to properly assess the impact of storage since decisions for charging/discharging involve temporal dependencies. Here, the second order cone program (SOCP) convex relaxation algorithm will be implemented using the same linear cuts in a multi-temporal application. The advantage of a multi-temporal problem formulation is the optimization of the charging and discharging schedule of a given time period, here between 12-96 consecutive time-steps.

The importance of multi-temporal coupling in an optimum power flow algorithm is directly related to the evaluation of the role of storage within an active distribution network. An alternative solution to curtailment on the RES generation is the storage of this energy in order to mitigate grid constraint violations. This stored energy can then be later used to minimize the high consumption peak periods. This multi-temporal coupling is critical in order to evaluate the technical constraints of the storage elements and the possible benefits. In this paper, an example active medium voltage distribution grid will be modeled in order to understand the existing RES hosting capacity with curtailment in comparison with centralized and decentralized storage options. This multi-temporal algorithm will allow the quantification of storage element advantages and their optimum placement.

II. Problem Formulation

A. Power Flow Model

Two different sets of equations can be used within a power flow model, the bus injection model (BIM) or the branch flow model (BFM). While both models can be effective for various applications, the BFM system of equations will be used due to better convergence characteristics as explained in [10] specifically in relation to a radial network topology. Let the labeled nodes i, j and k be oriented as described in the figure below.

$$node_i \xrightarrow[branch_{ij}]{} node_j \xrightarrow[branch_{jk}]{} node_k$$

When considering a radial distribution system with decentralized PV generation and decentralized storage elements, the power flow equations can be written as shown below.

$$P_{ij} = P_{load,j} + \sum_{k=1}^{n} P_{jk} + r_{ij} I_{ij}^2 + P_{pv,j} + P_{st,j} \tag{1}$$

$$Q_{ij} = Q_{load,j} + \sum_{k=1}^{n} Q_{jk} + x_{ij} I_{ij}^2 + Q_{pv,j} + Q_{st,j} \tag{2}$$

Equation (1) and (2) describe the balance of power from the upstream and downstream branches where P_{load}, P_{pv}, and P_{st} are respectively the instantaneous consumption, PV production and battery storage charge or discharge at a given timestep. P_{jk}, r_{jk}, Q_{jk},x_{jk} and I_{ij}^2 are respectively the power, the resistance, the reactive power, the reactance and the current associated with the branch *jk*. Q_{load}, Q_{pv}, and Q_{st} are respectively the instantaneous reactive consumption, PV reactive production, and battery reactive power values. The voltage at each node can be calculated by equation (3).

$$|V_j|^2 = |V_i|^2 - 2(r_{ij} P_{ij} + x_{ij} Q_{ij}) + (r_{ij}^2 + x_{ij}^2) I_{ij}^2 \tag{3}$$

where $|V_j|$ is the voltage magnitude at node *j*. The current of each branch is calculated as shown in equation (4).

$$I_{ij}^2 = \frac{P_{ij}^2 + Q_{ij}^2}{|V_i|^2} \tag{4}$$

B. System Constraints

The system constraints of an electrical distribution network include maximum and minimum voltage limits, maximum and minimum current limits, and operational limits imposed by individual components. The network voltage and current limits can be described as shown below:

$$\underline{V}_i \leq |V_i| \leq \overline{V}_i \tag{5}$$

where $\underline{V}_i$ and $\overline{V}_i$ are respectively the lower and upper limits of the voltage on a line. Individual components such as the PV and battery systems were modeled through their inverter behavior as described in the following sections.

1) PV Inverter Model: The PV inverter behavior was modeled as active and reactive generation source with upper and lower limits, $\overline{P}^{pv}$ and $\underline{P}^{pv}$ respectively on active power and $\overline{s}^{pv}$, $\underline{s}^{pv}$ on total apparent power injection for a given timestep.

$$\begin{aligned} \underline{P}_{pv} &\leq |P_{pv}| \leq \overline{P}_{pv} \\ \underline{s}_{pv} &\leq |s_{pv}| \leq \overline{s}_{pv} \end{aligned} \tag{6}$$

where s_{pv} is the total apparent power of the power injection as defined below.

$$\begin{aligned} s_{pv}^2 &= P_{pv}^2 + Q_{pv}^2 \\ s_{pv} &= \sqrt{P_{pv}^2 + Q_{pv}^2} \end{aligned} \tag{7}$$

2) Battery Inverter Model: The battery inverter was modeled as either a power injection or power consumption for a given node at a given timestep. The time coupling variable indicating the state of charge (SOC) was calculated based on a charging and discharging efficiency associated with the inverter.

$$\begin{aligned} E_{batt,t1} = E_{batt,t0} - \eta_{ch} P_{ch,t1} - \eta_{dch} P_{dch,t1} \\ P_{st} = P_{ch} + P_{dch} \\ \underline{s}_{st} \leq |s_{st}| \leq \overline{s}_{st} \end{aligned} \tag{8}$$

where η^{ch}, $P_{ch,t1}$, η_{dch}, $P_{dch,t1}$, $\overline{s}_{st}$ and $\underline{s}_{st}$ is the charging efficiency, power absorbed during charging, discharging efficiency, power injected into the grid, upper limit and lower limit of total apparent power exchange with the grid. P_{st} is the power injection or absorbed by the battery as defined below:

$$\begin{aligned} s_{st}^2 &= P_{st}^2 + Q_{st}^2 \\ s_{st} &= \sqrt{P_{st}^2 + Q_{st}^2} \end{aligned} \tag{9}$$

The power flow equations are non-linear and non-convex. Therefore, when solving a highly dimensional power flow problem, convex relaxation have been used to ensure high performance algorithms.

III. Optimum Power Flow Formulation

The same SOCP convex relaxation used in [19] and [17] is implemented in a multi-temporal model in order to analyze the hosting capacity of a distribution grid. This relaxation entails the relaxation of certain equality constraints and the substitution of certain quadratic terms for linear terms. The equality constraints in question, (4), (5) and (6), are relaxed ultimately relaxing the magnitude of currents within each branch and using a conic formation on the limitation of active power exchange with the grid. Two new variables are introduced to replace quadratic terms, $\upsilon_i = |V_i|^2$ and $\ell = |I_{ij}|^2$ in order to successfully formulate an SOCP problem as explained in [17].

A. Objective Function

In order to optimize the total system functionality, the objective function is composed of two parts. The first part is the minimization of the total losses of the system. The second part minimizes the curtailment of the PV systems in order to maximize renewable energy consumption within the grid. Therefore the objective function is formulated as seen below:

$$min \sum_{i=1}^{n} r_{ij}\ell_{ij} + (P_{ideal,i}^{pv} - P_i^{pv}) \tag{10}$$

B. SOCP Problem Formulation

The complete SOCP formulation is then found below:

$$min \sum_{i=1}^{n} r_{ij}\ell_{ij} + (P_{ideal,i}^{pv} - P_i^{pv}) \tag{11}$$

$$\begin{aligned} & s.t. \\ & (6), (7), (8), (9) \\ P_{ij} &= P_j^{load} + \sum_{k=1}^{n} P_{jk} + r_{ij}\ell + P_j^{pv} + P_j^{st} \\ Q_{ij} &= Q_j^{load} + \sum_{k=1}^{n} Q_{jk} + x_{ij}\ell + Q_j^{pv} + Q_j^{st} \\ \upsilon_j &= \upsilon_i - 2(r_{ij}P_{ij} + x_{ij}Q_{ij}) + (r_{ij}^2 + x_{ij}^2)\ell_{ij} \\ \ell_{ij} &\geq \frac{P_{ij}^2 + Q_{ij}^2}{\upsilon_i} \\ \underline{V}_i^2 &\leq \upsilon \leq \overline{V}_i^2 \end{aligned} \tag{12}$$

TABLE I
For a given timestep, the inexact instances present and calculation time in seconds

Timesteps coupled	Inexact instances	Calculation time (s)
12	0	33
12	2	38
48	0	121
48	18	158
96	0	289
96	36	339

IV. Algorithmic Performance

The optimization of storage elements and PV curtailment was analyzed for a time scale of 0.5 to 4 days. An example urban electric grid in France was studied in order to evaluate the performance of this algorithm. The network studied is a 30 kV 137 nodes typical urban grid topology. Network data was acquired through a partnership with ErDF. Twenty PV systems with equivalent power ratings were placed randomly throughout the grid topology with an associated battery system installed at the same node. The time of execution of the algorithm was recorded for varying time coupling scenarios as shown below.

This multi-temporal coupling allows the optimization of PV curtailment and battery storage utilization for up to a four day period with a satisfactory calculation burden. It also ensures that the relaxation is exact and applies linear cuts to timesteps that are not exact in order to guaranty the exactness of the relaxation.

V. Case Study

An example urban electric grid in France was studied to demonstrate possible algorithm utilization. The grid is composed of 137 nodes at 30 kV and serves as a medium voltage distribution grid feeder. A map of the grid topology can be found below.

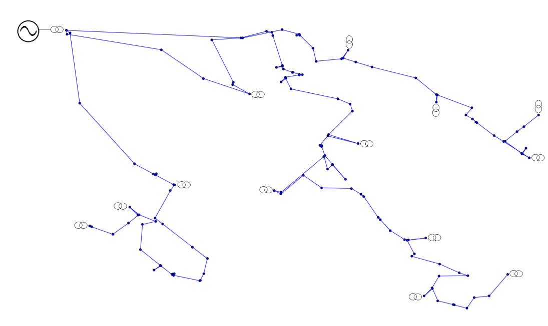

Fig. 1. Case study of typical medium voltage electric grid topology

Consumption load profiles were simulated using an aggregation load simulator as described in [20] for each low voltage substation and medium voltage consumer. This load simulator takes into account a mix of residential and commercial customers. Residential consumption is simulated with statistically accurate representations of surface area, electric heating and number of individuals that align with the INSEE building inventory database of France. Industrial load profiles are simulated by assuming a typical industrial activity mix in France from a medium voltage substation. The two medium voltage customers were modeled as office building complexes with typical business hours operation. A peak of 5 MW during the winter and 2.9 MW during the summer was simulated for the medium voltage substation transformer with a maximum apparent power limit of 10 MW. Solar radiation data from a site in the south of France was used to calculate expected PV production as a function of system nominal power.

Four different seasonal scenarios were studied in order to understand a typical annual operation. Within each season, three renewable energy solutions were studied: the hosting capacity of a typical grid topology without storage, the hosting capacity with decentralized storage elements installed at the same nodes as the PV systems and the hosting capacity with centralized storage elements close to the high voltage transformer. The hosting capacity of a feeder was defined as the maximum capacity of PV that does not violate grid constraints without using curtailment. Twenty sites were chosen for PV decentralized installations and nominal power of each system was increased until either current or voltage limits were reached.

VI. Results

A three day simulation period was chosen in order to allow for at least one full cycle of charging and discharging of the storage elements. Three day typical profiles were chosen for four different seasons in order to understand the annual performance of the system. Considering only PV installations without storage elements, the maximum current limit of the lines was reached during low loading periods and high peak PV injection in summer. Multiple capacities for 20 decentralized PV systems were tested until curtailment was necessary to not exceed voltage or apparent power limits of the network. The maximum installed capacity where curtailment was unnecessary was achieved with a PV penetration of 10 MW nominal power installed. A a total of 701 kWh of the 156 MWh produced during a three-day simulation was necessary to ensure maximum apparent power limits were not exceeded. During typical daily profiles for fall, winter and spring, no curtailment was necessary for a 10 MW systems. In all simulations, the summer period was the most critical to monitor for grid stability verification, therefore the rest of the results section will focus on summer production and consumption profiles. A comparison of the net consumption of the high voltage transformer and the total power injected into the high voltage grid from the medium voltage substation during summer periods can be found in figure 2.

The curtailment necessary and the losses on the lines were then compared as seen in figure 3.

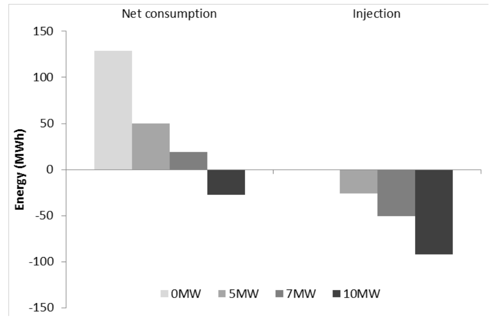

Fig. 2. Comparison of net consumption of feeder and total PV injection during a three day period using typical summer profiles

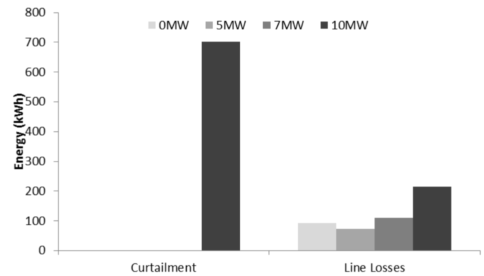

Fig. 3. Comparison of line losses of feeder and total PV curtailment necessary during a three day period using typical summer profiles

Added storage capacity was then integrated into the grid in order to quantify the additional hosting capacity possible. Initially storage elements were placed at the same nodes as all PV installations to represent a decentralized storage configuration. Therefore 20 systems of 116 kWh energy storage capacity were modeled through their inverter behavior as described in equation 8. For 10 MW of PV capacity installed, no curtailment was needed within all seasons. The improvement in system performance can be seen in figure 4 as a percentage increase or decrease for each parameter.

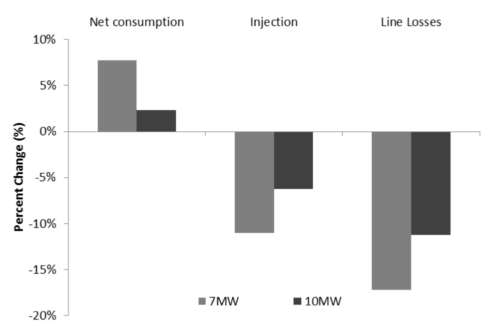

Fig. 4. Percentage increase or decrease due to added storage elemnts at each PV production node. Calculations for a 7 MW and 10 MW systems during a three days period using typical summer profiles

The same amount of storage capacity was then used in a centralized configuration. This centralized storage was placed very close to the high voltage transformer offering the same services. The necessary curtailement was also reduced to zero for the 10 MW system. However, the centralized battery system also resulted in higher overall line losses. The percentage change due to the presence of a centralized battery system is shown in figure 5.

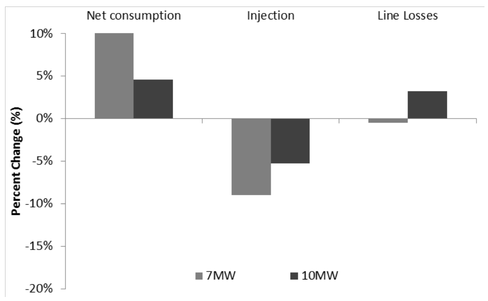

Fig. 5. Percentage increase or decrease due to an added centralized storage elemnt when comparing 7 MW and 10 MW systems during a three days period using typical summer profiles

VII. Conclusion

The optimization algorithm proposed in this paper successfully applied a convex relaxation algorithm with linear cuts to a multi-temporal application for battery storage analysis. This algorithm was shown to be effective when studying a distribution system for a 3-4 day time span. The multi-temporal algorithm allows for the assessment of battery storage functionality while taking into account the technology limitations such as charging and discharging efficiency, and maximum injection and absorption. The algorithm also calculates an optimal charging and discharging schedule based on the objective function. A French medium voltage distribution feeder was successfully analyzed to determine the hosting capacity, decentralized and centralized battery systems effects on curtailment. This algorithm could be used for comparison studies between different grid stability control strategies such as real time curtailment, centralized and decentralized battery installations. The use of this algorithm for real time management could also be effective if real time predicted PV production profiles and expected load profiles are used as inputs. The optimization of charging and discharging schedules of batteries can effectively increase hosting capacity of a distribution network by reducing the necessity to curtail PV systems.

Acknowledgment

The authors would like to thank ERDF for the provision of some of the data used in this study. Mr. Thibaut Barbier is thanked for his support with the simulated load curves. This work is performed in the frame of the European project Sensible (Grant Agreement 645963) funded in part by the European Commission under the Horizon 2020 Framework Program.

References

[1] A. Vinkovic, M. Suhadolc, and R. Mihalic, "Current-based models of {FACTS} devices for three-phase load-flow calculations using the newtonraphson method," *International Journal of Electrical Power & Energy Systems*, vol. 45, no. 1, pp. 117 – 128, 2013.

[2] D. R. R. Penido, L. R. de Araujo, S. C. Jnior, and J. L. R. Pereira, "A new tool for multiphase electrical systems analysis based on current injection method," *International Journal of Electrical Power & Energy Systems*, vol. 44, no. 1, pp. 410 – 420, 2013.

[3] M. Abdel-Akher, K. Nor, and A. Rashid, "Improved three-phase power-flow methods using sequence components," *Power Systems, IEEE Transactions on*, vol. 20, pp. 1389–1397, Aug 2005.

[4] X. Yang, Z. Wei, G. Sun, Y. Sun, Y. Yuan, Z. Lu, X. Xu, and L. Huang, "Power flow calculation for unbalanced three-phase distribution network with dgs based on phase-sequence hybrid modeling," in *Smart Energy Grid Engineering (SEGE), 2013 IEEE International Conference on*, pp. 1–6, Aug 2013.

[5] H. E. Farag, E. El-Saadany, R. E. Shatshat, and A. Zidan, "A generalized power flow analysis for distribution systems with high penetration of distributed generation," *Electric Power Systems Research*, vol. 81, no. 7, pp. 1499 – 1506, 2011.

[6] W. Wu and B. Zhang, "A three-phase power flow algorithm for distribution system power flow based on loop-analysis method," *International Journal of Electrical Power & Energy Systems*, vol. 30, no. 1, pp. 8 – 15, 2008.

[7] T.-H. Chen and N.-C. Yang, "Loop frame of reference based three-phase power flow for unbalanced radial distribution systems," *Electric Power Systems Research*, vol. 80, no. 7, pp. 799 – 806, 2010.

[8] N. Etherden and M. Bollen, "Increasing the hosting capacity of distribution networks by curtailment of renewable energy resources," in *PowerTech, 2011 IEEE Trondheim*, pp. 1–7, June 2011.

[9] S. Abdelouadoud, R. Girard, and T. Guiot, "Planning-oriented yearly simulation of energy storage operation in distribution system for profit maximization, voltage regulation and reserve provisionning," in *Electricity Distribution (CIRED 2013), 22nd International Conference and Exhibition on*, pp. 1–4, June 2013.

[10] L. Gan and S. H. Low, "Convex relaxations and linear approximation for optimal power flow in multiphase radial networks," in *Power Systems Computation Conference (PSCC), 2014*, pp. 1–9, Aug 2014.

[11] R. Madani, S. Sojoudi, and J. Lavaei, "Convex relaxation for optimal power flow problem: Mesh networks," in *Signals, Systems and Computers, 2013 Asilomar Conference on*, pp. 1375–1382, Nov 2013.

[12] M. Ghasemi, S. Ghavidel, M. Gitizadeh, and E. Akbari, "An improved teachinglearning-based optimization algorithm using lvy mutation strategy for non-smooth optimal power flow," *International Journal of Electrical Power & Energy Systems*, vol. 65, no. 0, pp. 375 – 384, 2015.

[13] S. Paudyal, C. Canizares, and K. Bhattacharya, "Three-phase distribution opf in smart grids: Optimality versus computational burden," in *Innovative Smart Grid Technologies (ISGT Europe), 2011 2nd IEEE PES International Conference and Exhibition on*, pp. 1–7, Dec 2011.

[14] X. Bai and H. Wei, "Semi-definite programming-based method for security-constrained unit commitment with operational and optimal power flow constraints," *Generation, Transmission Distribution, IET*, vol. 3, pp. 182–197, February 2009.

[15] J. Lavaei and S. Low, "Zero duality gap in optimal power flow problem," *Power Systems, IEEE Transactions on*, vol. 27, pp. 92–107, Feb 2012.

[16] S. Bose, S. Low, T. Teeraratkul, and B. Hassibi, "Equivalent relaxations of optimal power flow," *Automatic Control, IEEE Transactions on*, vol. 60, pp. 729–742, March 2015.

[17] M. Farivar, R. Neal, C. Clarke, and S. Low, "Optimal inverter var control in distribution systems with high pv penetration," in *Power and Energy Society General Meeting, 2012 IEEE*, pp. 1–7, July 2012.

[18] N. Li, L. Chen, and S. Low, "Exact convex relaxation of opf for radial networks using branch flow model," in *Smart Grid Communications (SmartGridComm), 2012 IEEE Third International Conference on*, pp. 7–12, Nov 2012.

[19] S. Y. Abdelouadoud, R. Girard, F.-P. Neirac, and T. Guiot, "Iterative linear cuts strenghtening the second-order cone relaxation of the distribution system optimal power flow problem," in *T D Conference and Exposition, 2014 IEEE PES*, pp. 1–4, April 2014.

[20] T. Barbier, R. Girard, F.-P. Neirac, N. Kong, and G. Kariniotakis, "A novel approach for electric load curve holistic modelling and simulation," in *MedPower 2014 - The 9th Mediterranean Conference on Power Generation, Transmission Distribution and Energy Conversion*, (Athènes, Greece), Nov. 2014.